INSTITUTE OF PHYSICS PUBLISHING MEASUREMENT SCIENCE AND TECHNOLOGY
Meas. Sci. Technol. **16** (2005) 183–190 doi:10.1088/0957-0233/16/1/024

A new design for high-throughput peel tests: statistical analysis and example*

Arnaud Chiche[1], Wenhua Zhang, Christopher M Stafford and Alamgir Karim

Polymers Division, National Institute of Standards and Technology, Gaithersburg, MD 20899-8542, USA

E-mail: arnaud.chiche@uni-bayreuth.de and chris.stafford@nist.gov

Received 28 April 2004, in final form 29 September 2004
Published 16 December 2004
Online at stacks.iop.org/MST/16/183

Abstract
The peel test is one of the most common techniques to investigate the properties of pressure sensitive adhesives (PSAs). As the demand increases for combinatorial tools to rapidly test material performance, designing a high-throughput peel test is a critical improvement of this well-established technique. A glaring drawback to adapting conventional peel tests to study combinatorial specimens is the lack of sufficient statistical information that is the foundation of this type of measurement. For example, using a continuous gradient of sample properties or test conditions in the peel direction implies that each data point (force) corresponds to a given test condition, thus prohibiting the average force to be calculated for a given condition. The aim of this paper is both to highlight the potential problems and limitations of a high-throughput peel test and suggest simple experimental solutions to these problems based on a statistical analysis of the data. The effect of the peel rate on the peel force is used to illustrate our approach.

Keywords: peel test, high-throughput, combinatorial methods, error bars, statistical treatment, force fluctuations, peel rate, debonding micro-mechanisms, pressure sensitive adhesives (PSAs)

M This article features online multimedia enhancements

(Some figures in this article are in colour only in the electronic version)

1. Introduction

Peel tests continue to be the industrial 'standard' to assess the properties of pressure sensitive adhesives (PSAs) (Satas 1989). The adhesives industry would be served broadly by a measurement platform that is amenable to high-throughput approaches, as it would decrease the labour intensive and time-consuming sample-by-sample testing, as well as enable researchers to more thoroughly explore the largely uncharted parameter space associated with adhesive systems. Yet there are considerable technical challenges presented by adapting conventional peel tests to include combinatorial or high-throughput approaches.

Generally, a peel test involves measuring the applied load required to remove an adhesive tape from a substrate under displacement control. In a conventional peel test, both the adhesive tape and the substrate are homogeneous, and the test is performed with constant condition parameters such as the peel angle, the peel rate or the temperature. One might expect the applied force to be constant as a result of the constant conditions and parameters. In fact, this is never the case even in a conventional test without macroscopic stick–slip, i.e., the measured force presents notable fluctuations. For this discussion, we ignore the possibility of stick–slip at the peel front and the characteristic force oscillations associated with this mechanism.

* Official contribution of the National Institute of Standards and Technology; not subject to copyright in the United States.
[1] Present address: Universität Bayreuth, Physikalische Chemie II, 95440 Bayreuth, Germany.

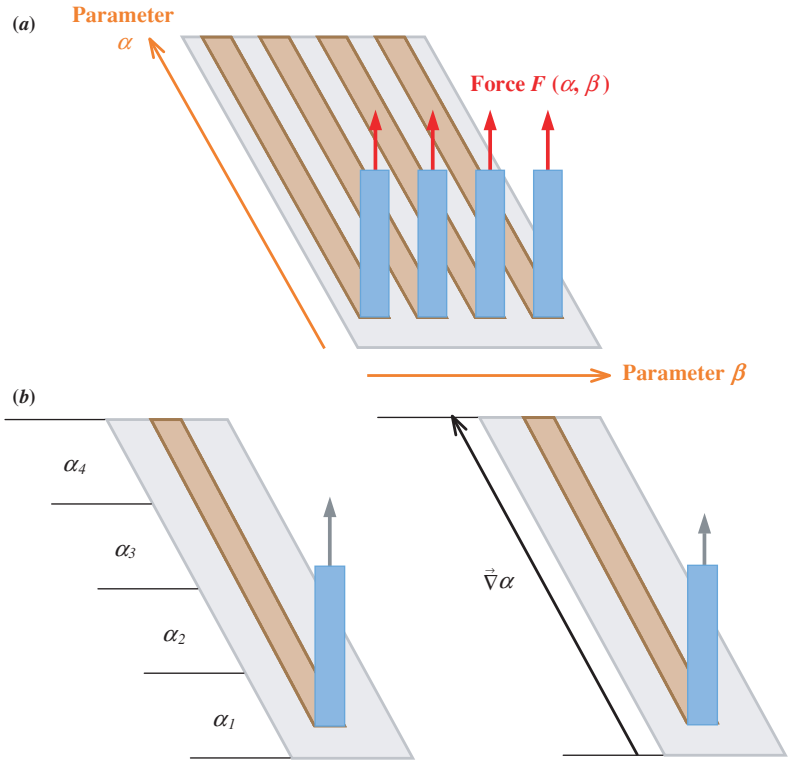

Figure 1. (*a*) Schematic of a combinatorial peel test, or how one can quickly measure the dependence of the peel force F with two parameters α and β; (*b*) Discrete (left) or continuous (right) variation of an experimental parameter α along the peeling direction.

The origin of these fluctuations is poorly understood: it can occur as a result of uncontrollable variability in the sample properties (sample heterogeneities at a small scale) or the peel conditions, or due to microscopic heterogeneities in the mechanisms involved in the debonding process. Even without a macroscopic stick–slip, the peeling of an adhesive tape happens by various combinations of pure crack with finger instabilities (Verdier *et al* 1998, Urahama 1989, Ghatak *et al* 2000), interfacial sliding (Zhang-Newby and Chaudhurry 1997, Amouroux *et al* 2001) and cavitation (McEwan 1966, Urahama 1989). The scale of these mechanisms is controlled by the thickness of the adhesive layer (typically from 10 μm to 100 μm) and is therefore generally much smaller than the tape width (centimetre scale). Even at a scale that is small compared to the tape width, heterogeneities are able to produce peel force fluctuations of variable amplitude. The standard treatment to remove the force fluctuation in a conventional peel test (ASTM 1999) simply consists in calculating the average value $\langle F \rangle$ of the peel force and the associated uncertainty $\Delta\langle F \rangle$ (the standard deviation of the average calculation, for example).

We now consider a high-throughput peel test, as shown schematically in figure 1(*a*). The motivation behind this high-throughput experimental design is to obtain complete dependence of the peel force F on two independent parameters (α and β in figure 1(*a*)) from a single test. The effect of parameter β is accessible through several peel tests performed simultaneously, each with different average values of β, and the use of several individual load cells to measure independently the force applied on each tape. Although this design is technically feasible, we will not focus on it since it is not fundamentally different from a conventional test (one can treat each of the resulting force curves as a single test). We will focus instead on the case of a systematic variation of the parameter α in the peeling direction. The variation of this parameter can be discrete (figure 1(*b*), left) with short homogeneous domains or continuous (figure 1(*b*), right) with the use of a gradient of α. In both cases, the force will no longer be constant (assuming a measurable sensitivity to the parameter α) and consequently the simple analysis for calculating an average peel force $\langle F \rangle$ (mentioned above for a conventional test) is no longer valid. For discrete variations of parameter α, the domain size could be too small to obtain an accurate average value of the force, and by definition a continuous variation of the parameter prevents an average calculation even being made (only one force measurement per parameter value). Under these conditions, a high-throughput peel test can be used as a screening test at best, and due to poor statistics fails as a replacement for conventional quantitative tests.

In this paper, we propose to develop and apply a statistical treatment of the peel data based on an analysis of a standard test (macroscopically homogeneous sample and conditions). After an experimental section describing the sample preparation and the main theme of the set-up, a treatment of the force fluctuations will be presented. As an illustration, we apply our treatment to a simple study of the effect of the peel rate on the peel force and the debonding micro-mechanisms.

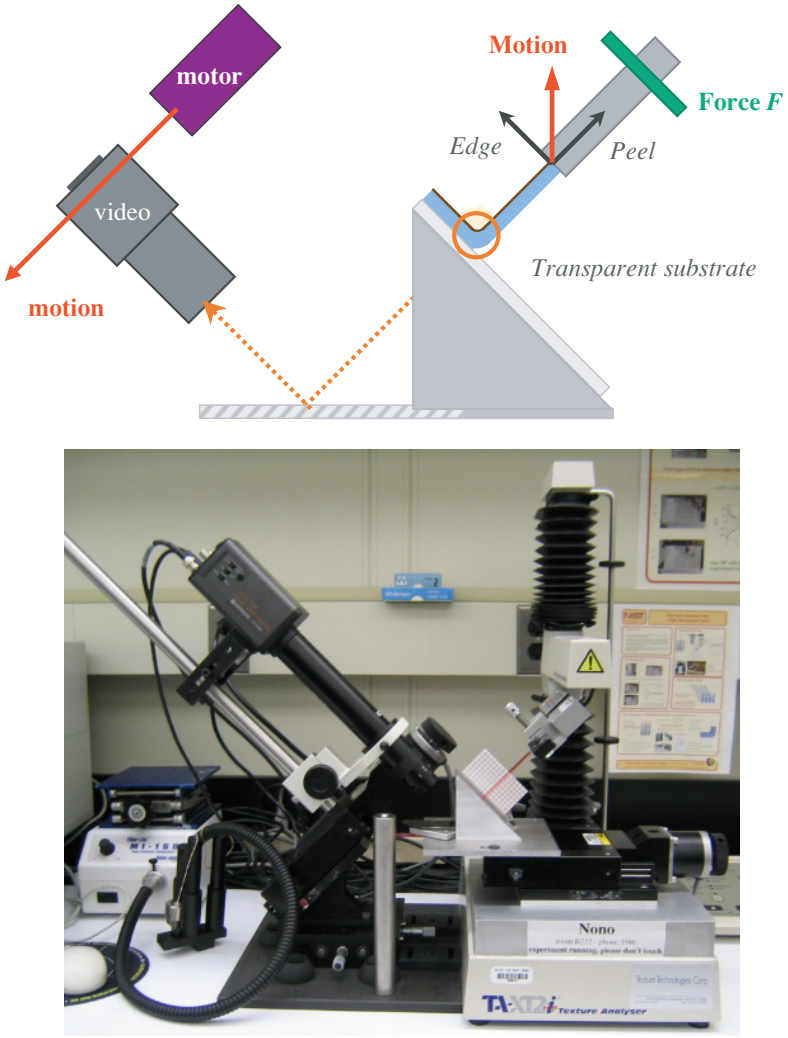

Figure 2. Schematic (top) and picture (bottom) of the custom-designed experimental set-up used for both conventional and high-throughput peel test experiments.

2. Experimental design and set-up

We perform 90° peel experiments with a custom-designed apparatus (figure 2) built around a commercial tensile machine (TA.XT2i Texture Analyzer, Texture Technologies Corp., Scarsdale, NY/Stable Micro systems, Godalming, Surrey, UK). A key feature of this new design is that it allows for simultaneous measurement of both the force F (1 mN resolution) applied during the peel of the tape at a given rate (between 7 μm s^{-1} and 7 mm s^{-1}), and images of the contact edge through the transparent substrate (adherent). In addition, the instrument allows a correlation between the force and the images as the imaging system follows the peel front during the test.

The imaging system[2] has two major purposes. First, it affords us the ability to study the debonding mechanisms (fingering, sliding and cavitation) at a micro scale. Such an optical probe has been successfully used to characterize and understand these mechanisms in different geometries (see references given in the introduction for peel test; Creton and Fabre (2002) and reference therein for more confined geometries). Furthermore, the real time imaging system is an efficient means to measure and/or control the effective peel rate. For example, if the peel front and the camera are moving at the same rate, the peel front will appear static in the recorded images. On the other hand, since there is no mechanical connection between the camera motion and the peel motion (figure 2), any variation of the effective peel rate (e.g., due to a stretching of the tape) will result in an apparent motion of the peel front in the images. The rate of this apparent motion is directly related to the difference between the nominal and the effective peel rate, and thus a real time peel rate measurement can be performed.

We used two office adhesive tapes: a translucent removable one, A (Scotch 811, 3M) and a transparent one, B (Scotch 600, 3M). These tapes have been applied on glass adherent surfaces at room temperature with a commercial 2 kg (4.5 lb) roller (diameter 9.5 cm and width 4.5 cm, ChemInstruments, Inc.). The glass substrate was previously wiped with acetone and dried with nitrogen. The peel test was performed within a few minutes of the application to the adherent, at room temperature in the experiments reported

[2] An example movie can be download from ftp://ftp.espci.fr/shadow/Arnaud/ (∼10 Mb, format DivX) or is available on demand.

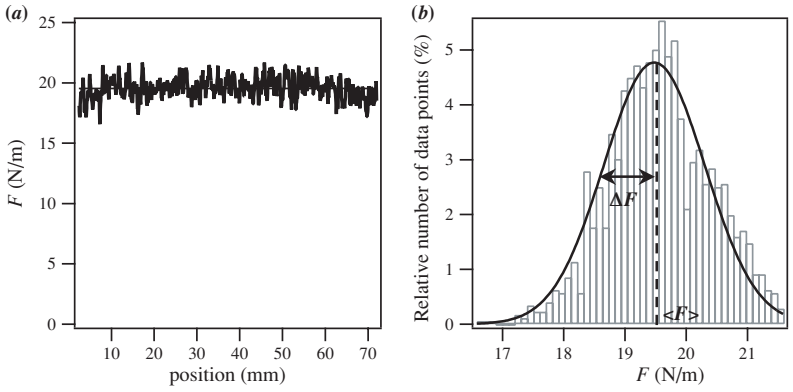

Figure 3. (*a*) Peel force F versus position curve from a conventional peel experiment (removable adhesive A peeled from a glass surface at 1 mm s^{-1}; (*b*) Gaussian distribution of these data points.

here. Note that the force is normalized by the tape width (19 mm in all cases), so that the peel force F is given in units of N m^{-1} (or J m^{-1} that corresponds to a debonding energy per unit surface area).

3. Statistics of a conventional peel test

We start with the statistical analysis associated with a conventional peel test (figure 3(*a*)). The tape is the removable adhesive A (see above) peeled from a regular glass substrate at 1 mm s^{-1}. Under these conditions, the average peel force $\langle F\rangle$ is 19.53 N m^{-1} (calculated from equation (1) where i is associated with a data point and $N = 1758$ the number of data points) and the uncertainty $\Delta\langle F\rangle$, corresponding to the standard deviation of the average calculation (standard deviation σ divided by the square root of the number N of points, equation (2)), is 0.02 N m^{-1} (0.1%). Despite this very small uncertainty (same order of magnitude as the load cell resolution), one can notice much bigger fluctuations of the force F (values spread in a 5 N m^{-1} wide range). These fluctuations can be quantified through the distribution of the values. Figure 3(*b*) represents a histogram of the density n of measurement points at the different force values F. These data can be approximated by a Gaussian distribution (equation (3)).

$$\langle F\rangle = \frac{1}{N}\sum_{i=1}^{N} F_i \tag{1}$$

$$\Delta\langle F\rangle = \frac{\sigma}{\sqrt{N}} = \sqrt{\frac{\sum_{i=1}^{N}(F_i - \langle F\rangle)^2}{N\,(N-1)}} \tag{2}$$

$$n(F) \propto \exp\left[-\frac{(F-\langle F\rangle)^2}{2(\Delta F)^2}\right]. \tag{3}$$

It follows that the average value $\langle F\rangle$ calculated from the previous linear fit (figure 3(*a*)) is the centre of the Gaussian distribution. The Gaussian fit of the data also provides a distribution width ΔF (equal to the standard deviation σ), calculated here to be 0.85 N m^{-1} (4.4% of the average value). This parameter quantifies the scatter of the measured values F_i around the average value. In other words, if one determines the force with a single data point, the uncertainty is of the order of ΔF (about 4.4%). If now the average peel force is determined from a large data set (figure 3(*a*) for example), the uncertainty $\Delta\langle F\rangle$ becomes much smaller (0.1%). Now, let us consider what would happen if we calculate the average force from an intermediate number of data points. The uncertainty in this calculation will obviously depend on the number of data points included in the calculation. A simple solution would involve calculating the average value $\langle F\rangle$ using an increasing number of successive points from the initial set of data (figure 3(*a*)). A plot of the average value versus the number of points used (or in other words, the length of tape L for the average calculation[3]) would help us to address this problem. Due to the force fluctuations, the position of the set of data points can affect the calculated average value (obviously if one considers the extreme case of a unique datum, the result will depend on the position of this datum, and a broad range of values can be obtained). As our purpose is to characterize these force fluctuations and how they vary with the length L of the tape, it is crucial to vary the position of the set of data points used for the average calculation.

We present in figure 4(*a*) the result of the average force calculation based on 100 different data set positions (uniformly distributed along the total range in figure 3(*a*)). By 'position' we mean the centre of the domain used for the average calculation. For each of these positions, the size of the data domain (i.e., the number of points taken into account) has been increased from zero (average value equal to the value of the domain centre data point) to a maximum size (when the domain used for calculation reaches one edge of the whole set of data points). Each domain position is then associated with one of the thin grey curves in this average force versus domain size representation.

Figure 4(*a*) can be interpreted as follows: for a given length of tape L used for the average force calculation, the result should be within the range of values between the extreme values of the previous calculation (black points on figure 4(*a*)). The difference between these two black curves then represents twice the error bar $\Delta\langle F\rangle$, as illustrated in figure 4(*a*) for a 20 mm length L. Figure 4(*b*) finally represents the uncertainty $\Delta\langle F\rangle$ of the average calculation as a function of the length L

[3] In all the experiments we report in this paper, the force has always been measured at constant time interval. As the peel rate has been constant, two consecutive data points are always separated by the same distance δL covered by the peel front (39.6 μm in the experiment associated with figures 3 and 4, 2.8 μm for figure 5).

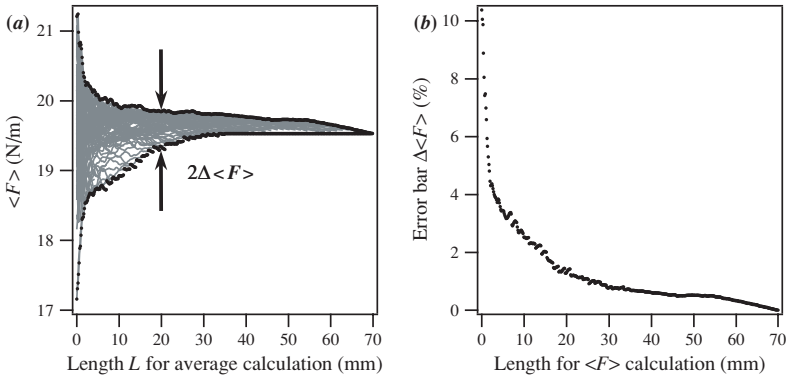

Figure 4. (*a*) Average value of the peel force calculated from figure 3(*a*) over 100 domains centred on different positions (each thin curve results from a given position). The dotted curves highlight the extreme values of the average calculation according to the domain size (as underlined by the arrows); (*b*) Uncertainty $\Delta\langle F\rangle$ of the average peel force as a function of the length for calculation.

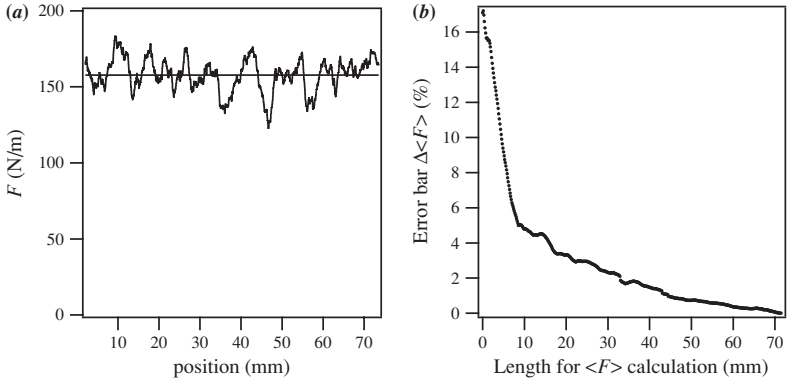

Figure 5. (*a*) Peel force F versus position curve from a conventional peel experiment (adhesive tape B removed from a glass surface at 35 μm s^{-1}); (*b*) Uncertainty $\Delta\langle F\rangle$ of the average peel force as a function of the length for calculation.

of the tape used for the calculation. As the length L of the tape increases from zero to 70 mm (the length of our homogeneous sample), the uncertainty in the average force decreases from about 10% to zero. It is important to note that this is only related to the effect of a limited sample length; in all cases one has to also consider the uncertainty given by the average calculation itself (the standard deviation $\Delta\langle F\rangle$ of the calculation, equation (2)) that can be the limiting factor.

It is interesting to conclude this section with an application of this statistical treatment to the other adhesive tape, B. Figure 5 represents the force versus position (5(*a*)) and the uncertainty $\Delta\langle F\rangle$ versus the sample length L (5(*b*)) obtained from a conventional peel test at a rate of 35 μm s^{-1}. This stronger adhesive (average force $\langle F\rangle$ about 158.85 N m^{-1} $\pm$ 0.07 N m^{-1}, the small uncertainty resulting from the important number of points) presents larger fluctuations (Gaussian distribution width $\Delta F = 9.2$ N m^{-1}, i.e., $\cong 5.8\%$), which results in higher values for the average force uncertainty $\Delta\langle F\rangle$ (figure 5(*b*)). The sensitivity of this uncertainty to experimental parameters, especially the adhesive, is currently under investigation.

4. Application: effect of peel rate

As a practical application of this statistical treatment to a high-throughput peel test, we present a brief study of the peel rate effect on the separation force. Many experimental parameters can be investigated this way, including those related to the substrate properties (Chiche *et al* 2004).

For this study, we performed a four-step test on a single sample (adhesive tape applied to a homogeneous glass slide), each step being performed at a different peel rate (from 7 μm s^{-1} to 7 mm s^{-1}). In fact, for the illustration purpose, these are four short but individual tests performed one after the other (about a minute between two successive steps). The measured force versus position is presented in figures 6(*a*) and 7(*a*), respectively for adhesive A (Scotch 811) and adhesive B (Scotch 600). One can note an initial overshoot in the force (relative to the plateau) at the start of each step. Analogous to an inertial effect, the overshoot increases with the peel rate, and is generally related to initiation of the adhesive tape shear and to changes in the peel front shape. We will not discuss this point further as it is out of the scope of the present paper; we direct the reader to a later communication on this issue.

For each of these steps, an average peel force was calculated from the plateau region. A domain length L was then associated with each average value, and by using the previous statistical characterization we are able to associate an error bar $\Delta\langle F\rangle$ for each of the resulting experimental values $\langle F\rangle$. It is important to highlight a limitation of this statistical treatment. As mentioned earlier, the force fluctuations and the resulting error bar curves (figures 4(*b*) and 5(*b*)) are expected to be potentially sensitive to the experimental parameters and

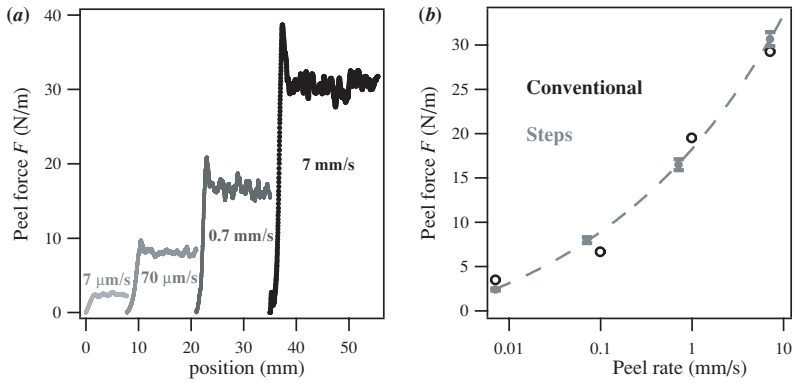

Figure 6. (*a*) Force versus position during a four-step peel test at different rates (removable adhesive A); (*b*) Force versus peel rate curve from this step test (filled grey circles) compared with four conventional tests (open black circles). The error bars are obtained from figure 4(*b*) and from the standard deviation of the average calculation (equation (2)), respectively.

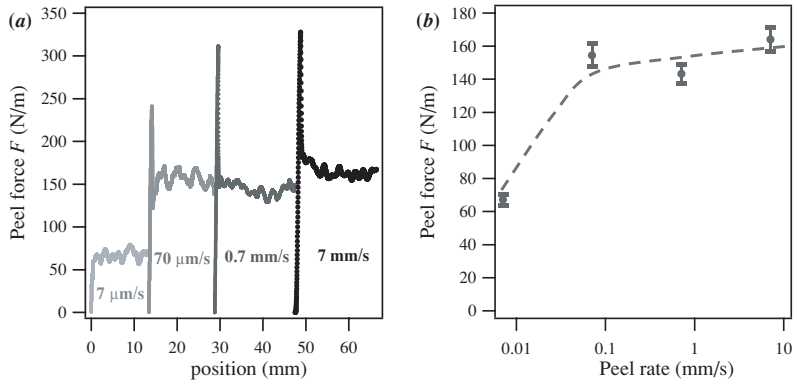

Figure 7. (*a*) Force versus position during a four-step peel test at different rates (adhesive B); (*b*) Force versus peel rate curve from this step test. The error bars are obtained from figure 5(*b*).

conditions (including the adhesive and the peel rate). As a result one should consider performing a conventional test for each experimental condition (in this case the peel rate) to get an accurate uncertainty value for the force. A high-throughput test then appears either not necessary or not possible as one first needs to perform all the associated conventional tests. Fortunately we will not end with such a negative conclusion, and we still consider a high-throughput peel test possible. The key to this problem is the amplitude of the studied effect and how accurate the experimental results have to be. First it is important for the amplitude of the studied effect to be larger than the uncertainty of the measurement. We also have to keep in mind that screening is the main purpose of a high-throughput experiment, to quickly get either a characterization of some properties or an approximate parameter range for a specific behaviour. In this context a high accuracy of the error bars is not that important, and it seems reasonable to get the error bar for each step from a single conventional test (homogeneous sample and conditions) performed on a given tape. The statistical analysis we propose is useful and sufficient.

In the peel rate example presented here we chose to use the uncertainty curves (figures 4(*b*) and 5(*b*)) from a single condition. The resulting curves $\langle F \rangle$ (v) are shown in figures 6(*b*) and 7(*b*), respectively, for adhesives A and B. One can see from the data for the removable tape A (figure 6(*b*)) a remarkably good agreement between the high-throughput and the conventional tests.

Even if the high-throughput 'step test' has a higher uncertainty, it is far from hiding the peel rate effect, which we are still sensitive to. The removable adhesive tape A (figure 6(*b*)) exhibits a regular increase of the force as a function of the peel rate (log scale). This typical behaviour is usually related to the viscoelastic properties of soft adhesive materials (Satas 1989), with a glass transition temperature T_g which is 50 °C to 70 °C below room temperature: increasing the rate has similar results as decreasing the temperature, meaning increasing the viscous dissipation as the system gets closer to its T_g (tan δ increases). The case of adhesive tape B (figure 7(*b*)) is slightly different. If an increase of the force with the peel rate is obvious between 7 μm s^{-1} and 70 μm s^{-1}, the peel force appears insensitive to the rate above this value. One can suspect a change in the rate-dependent behaviour around 70 μm s^{-1}. It is important to properly analyse these mechanical data to relate them to the debonding mechanisms as obtained by image analysis of the peel front through the substrate.

4.1. Image input

The study of the rate effect on the peeling of these adhesive tapes can be completed with an observation of images taken either during the test (real time) or after the test (post-mortem). Figures 8 and 9 show images associated with the removable tape A and with the tape B, respectively. Only images associated with the three slower tests are shown here, the

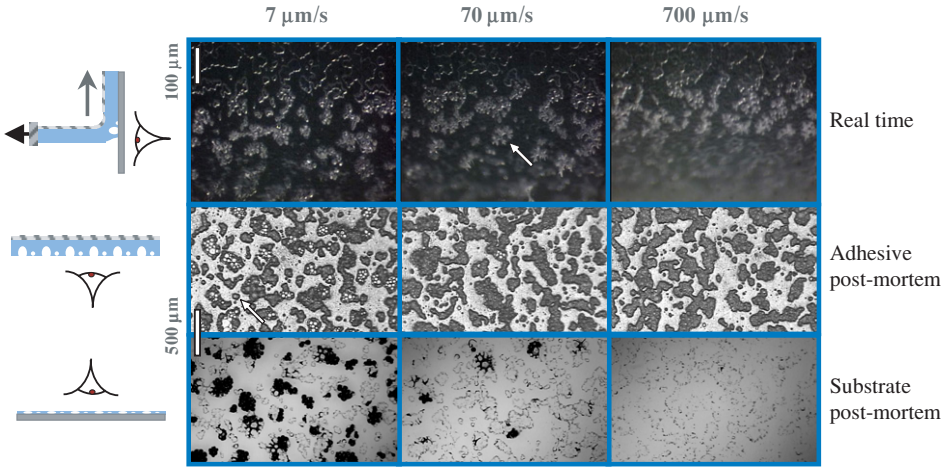

Figure 8. Images from the step test of the removable adhesive tape A at different peel rates as indicated.

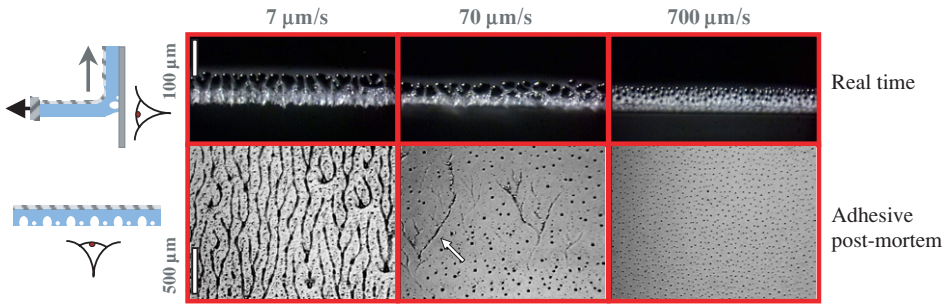

Figure 9. Images from the step test of the adhesive tape B at different peel rates as indicated.

faster tests (7 mm s^{-1}) being too fast for our current real time imaging system. Both real time and post-mortem images are oriented with the peel direction from the bottom to the top of the images. This means the top of the real time images is still in contact while the bottom is no longer in contact. It is important to note that all the tests we present in this study have been performed without fluorescent dyes, so that we are not directly imaging interfacial sliding phenomena, and we do not discuss this potential mechanism for this reason.

The images in figure 8 are associated with the step test of the removable tape A. The adhesive layer is not homogeneous, but made of micro-spheres (diameter about 50 μm). These sticky particles can be isolated (as indicated by the arrow on the left middle image) or a few of them can be flocculated to form adhesive spots of about 200 μm size. This design implies a very limited adhesive/substrate contact (top of the top images) that partly explains the moderate peel force, and this structure results in a light-diffusive tape (translucent but not transparent).

The debonding of the tape occurs by stretching these independent spots of adhesive material until they detach from the substrate. First, the surface of the contact spot decreases during the stretching with a finger-like crack propagation. One can see the star-shape of these contacts indicated by the arrow on the middle of the top images of figure 8. Subsequently the adhesive fibril detaches from the substrate by fracture, either at the interface ('adhesively') at 700 μm s^{-1}, or in the fibril ('cohesively') at 7 μm s^{-1}. These different types of behaviour can be detected both from real time or post-mortem images of the adhesive tape (figure 8, second row of images) or the substrate (figure 8, bottom row of images). Residual adhesive spots removed from the tape can be seen on the substrate after the separation at low rate (left) but not at higher rate (right). Obviously this office tape is not designed to be removable for such a slow peel. It is interesting to note that such a transition cannot be detected on the force versus rate curve (figure 6(*b*)), but is obvious in the images.

The images corresponding to the test of the other tape (B) are very different, both for real time and for post-mortem observations (figure 9), as well as the contact structure and the mechanisms involved. What is similar, as we show below, is that a rate-driven transition in the debonding mechanisms can be observed. The adhesive layer in this case is homogeneous, and the contact with the substrate is complete (at least at a micro-scale). All the mechanisms occur at the edge of this contact (peel edge) in about a 100 μm width domain (mainly controlled by the adhesive layer thickness as shown by Kaelble (1965)).

At the lowest rate (7 μm s^{-1}, left images), the debonding mainly occurs by finger-like crack propagation. As the fingers propagate, the adhesive walls between them are stretched at the back of the edge (fibrillation) before they eventually adhesively separate from the substrate (no residual adhesive is left on the substrate). This stretching of the viscoelastic

adhesive induces plastic deformation, leaving behind on the tape a pattern made of lines (bottom left image of figure 9). As the peel rate increases, the energy cost associated with this crack propagation increases due to the viscoelastic nature of the adhesive material (Maugis and Barquins 1978). At 70 μm s^{-1} (middle images), the fingers start splitting a lot, leaving a branching pattern as pointed out by the arrow on the bottom middle image. Cavitation eventually becomes the primary mechanism of failure (spots left on the tape after the test). At 700 μm s^{-1} (right images) and above, the debonding exclusively occurs by the growth of many small cavities.

These results show that the debonding mechanism of adhesive B exhibits a rate-driven transition from fingering (crack propagation) to cavitation. Unlike the 'cohesive to adhesive' transition exhibited by the removable adhesive A, this transition can be detected from the force versus rate curve (figure 7(*b*)). As previously mentioned for this tape, the force increases with the rate for slow peel tests associated with crack propagation but appears to be insensitive to the rate when the debonding is driven by a cavitation mechanism.

The images taken during or after the test allow us to highlight the possible transitions of the debonding mechanisms (cohesive to adhesive separation, finger-like crack to cavitation, etc . . .) that have to be taken into account when studying the evolution of the peel force with some parameter.

5. Conclusion

We focused in this work on the ability of a high-throughput peel test to respond to the increasing demand for fast screening experimental methods. More than a simple demonstration of the ability of the proposed design, this work underlined the important question of the statistical analysis of the data. We have proposed a new statistical tool for better high-throughput adhesion tests. This tool is simple and easy to apply, and is efficient as the example of the peel rate effect has shown. Even though it has been exclusively applied here to the peel test, the same treatment can also be useful for other mechanical tests that can exhibit a fairly high uncertainty.

As an extension of the initial goal of this work, this statistical analysis can also be used to quantify the level of noise of the experiment, as well as improve the experimental set-up or the sample preparation and analyse the debonding mechanisms through their effect on the peel force fluctuations.

Finally the short study of the peel rate effect highlights the efficiency of an imaging system to study the debonding mechanisms and correlate these with the force variations. Since the imaging field of view is small enough to be sensitive to these mechanisms but large enough to follow many of these simultaneously, image analysis can provide additional statistical information as well as a significant value for interpreting data from high-throughput experiments.

Disclaimer

Certain commercial materials and equipments are identified for adequate definition of the experimental procedures. In no instance does such identification imply recommendation or endorsement by NIST that the material or equipment is necessarily the best available for the purpose.

Acknowledgments

We would like to thank Patricia McGuiggan for helpful advice and discussions, James Filliben and Kevin Van Workum for suggestions regarding statistical analysis and Peter Votruba-Drzal for useful comments.

References

Amouroux N, Petit J and Léger L 2001 Role of interfacial resistance to shear stress on adhesive peel strength *Langmuir* **17** 6510

ASTM 1999 Standard test method for peel or stripping strength of adhesive bonds *ASTM Standard* 903-98

Chiche A, Zhang W and Stafford C M 2004 Peel test revisited using novel high throughput methods *Proc. 27th Ann. Meeting of the Adhesion Society* pp 42–3

Creton C and Fabre P 2002 TACK *Comprehensive Adhesion Science* vol II

Ghatak A, Chaudhury M K, Shenoy V and Sharma A 2000 Meniscus instability in a thin elastic film *Phys. Rev. Lett.* **85** 4329

Kaelble D H 1965 Peel adhesion: micro-fracture mechanics of interfacial unbonding of polymers *Trans. Soc. Rheol.* **9** 135

Maugis D and Barquins M 1978 Fracture mechanics and the adherence of viscoelastic bodies *J. Phys. D: Appl. Phys.* **11** 1989

McEwan A D 1966 The peeling of a flexible strip attached by a cavitating viscous adhesive *Rheol. Acta* **5** 205

Satas D 1989 *Handbook of PSA Technology* 2nd edn (New York: Van Nostrand Reinhold)

Urahama Y 1989 Effect of peel load on stringiness phenomena and peel speed of pressure-sensitive adhesive tape *J. Adhesion* **31** 47

Verdier C, Piau J-M and Benyahia L 1998 Peeling of acrylic pressure sensitive adhesives: cross-linked versus uncross-linked adhesives *J. Adhesion* **68** 93

Zhang Newby B-M and Chaudhurry M K 1997 Effect of interfacial slippage on viscoelastic adhesion *Langmuir* **13** 1805